



Title	Strong Ground Motion from the Urakawa Earthquake of Jan. 25, 1989
Author(s)	Mahdavian, Abbas; SASATANI, Tsutomu
Citation	Journal of the Faculty of Science, Hokkaido University. Series 7, Geophysics, 9(2), 253-267
Issue Date	1992-02-29
Doc URL	<a href="http://hdl.handle.net/2115/8787">http://hdl.handle.net/2115/8787</a>
Type	bulletin (article)
File Information	9(2)_p253-267.pdf



[Instructions for use](#)

# Strong Ground Motion from the Urakawa Earthquake of Jan. 25, 1989

Abbas Mahdavian and Tsutomu Sasatani

*Department of Geophysics, Faculty of Science,  
Hokkaido University, Sapporo 060, Japan*

( Received November 14, 1991 )

## Abstract

A moderate size earthquake ( $M=5.8$ ,  $H=49$  km) occurred on Jan. 25, 1989 beneath Urakawa, southern part of Hokkaido. Strong ground motions during this earthquake were well recorded by 10 accelerographs and 2 velocity-type strong motion seismographs. The recorded peak accelerations range from 320 down to 1 cm/sec<sup>2</sup>, depending on epicentral distances from 4 to 350 km respectively. In this paper, we studied the source, propagation path and site effects based on these strong motion records. First the seismic moment was estimated from the area of the first P pulses at near stations with the epicentral distance less than 100 km. Next we obtained acceleration spectra for transverse and radial components and interpreted the spectral shapes at high frequencies based on the  $\omega$ -square model, the spectrum of S-wave acceleration. Most spectral shapes obtained are similar to the  $\omega$ -square model, but some deviate from this model; the latter shows the sharp peak at about 2 or several Hz which may be attributed to site resonances. We observed the other site effects: Strong excitation of long-period seismic waves (0.5 Hz) after S arrivals at stations located in alluvial plain having thick sedimentary layers. These waves may be surface waves locally generated on the irregular, sediment-basement interface. Finally we obtained the quality factors of S waves at several frequencies, assuming that geometrical spreading causes a  $r^{-1}$  decay in spectral amplitudes; the quality factors increase with frequency.

## 1. Introduction

The  $M=5.8$  Urakawa earthquake occurred beneath Urakawa on Jan. 25, 1989. The hypocenter is: longitude 142.79°E, latitude 42.12°N, and a depth of 49 km (after JMA). This earthquake is one of the strongest earthquakes to have occurred in Urakawa area, in the south of Hokkaido, since the 1982 Urakawa Oki earthquake ( $M=7.1$ ). The 1989 Urakawa earthquake was well recorded by 10 strong motion accelerographs and 2 velocity-type strong motion seismographs. Figure 1 shows locations of the 1982 and 1989 Urakawa earthquakes and instrument locations that recorded the strong ground motion from the 1989

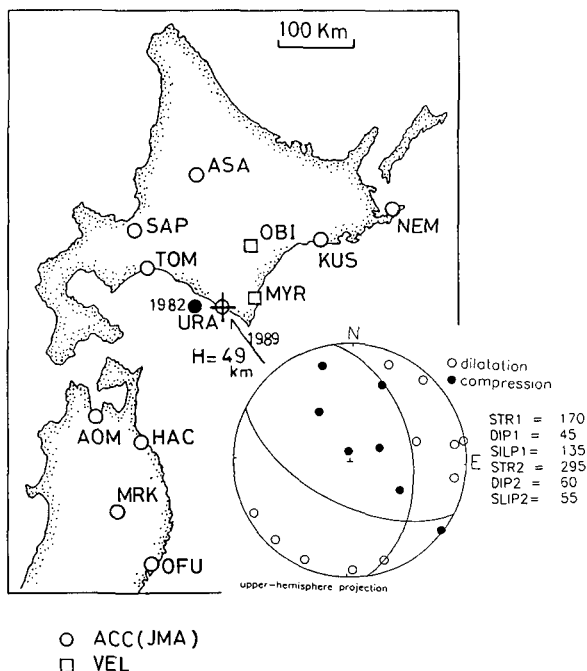


Fig. 1. Epicenters of the 1982 and 1989 Urakawa earthquakes and stations recorded strong ground motion from the 1989 earthquake. The focal mechanism of the 1989 earthquake is also shown.

earthquake. The Urakawa area being at the west side of the Hidaka Mountains in southern Hokkaido, is located near the junction of the Kuril and Northeastern Japan arcs.

The physical processes of strong ground motion that control the ground motion are generally separated into three parts: the excitation of seismic waves at the earthquake source; the effects of the Earth structure on the propagation of these waves including geometrical spreading, dispersion, scattering and attenuation; and the local site effects, that is, scattering and amplification due to topography and surficial geology. In this paper, we study some of these effects on ground motion by analyzing strong motion records from the 1989 Urakawa earthquake.

## 2. Data

The data consist of ten three-component digital accelerograms recorded by

Table 1. Stations used in this analysis.

Station name	Dis. km	Azim. deg.	$A_{\max}$ cm/s <sup>2</sup>		$V_{\max}$ cm/s		Instrument type
			Trans.	Radial	Trans.	Radial	
URA (Urakawa)	4.0	350	300.08	167.13	20.23	10.74	A
MYR (Moyori)	46.0	66	13.65	7.93	1.20	0.80	V
OBI (Obihiro)	90.0	21	13.31	15.40	1.58	1.45	V
TOM (Tomakomai)	114.6	300	11.88	11.71	0.75	1.00	A
SAP (Sapporo)	158.8	311	3.82	4.82	0.32	0.40	A
KUS (Kushiro)	162.3	53	8.63	5.80	0.30	0.28	A
ASA (Asahikawa)	186.5	349	1.18	1.20	0.16	0.16	A
HAC (Hachinohe)	206.4	211	7.89	9.03	0.30	0.30	A
AOM (Aomori)	221.5	229	9.70	6.30	0.40	0.38	A
NEM (Nemuro)	265.8	58	0.63	1.07	0.04	0.08	A
MRK (Morioka)	302.5	207	2.96	4.32	0.16	0.25	A
OFU (Ofunato)	351.6	195	1.58	1.52	0.06	0.04	A

$A_{\max}$ =maximum acceleration,  $V_{\max}$ =maximum velocity, A=accelerograph, V=velocity-type strong motion seismograph.

JMA servo-type accelerometer, and two three-component digital velocity seismograms recorded by us (Sasatani et al., 1990). The signals are digitized at JMA stations by a sampling frequency of 50 Hz and with a dynamic range of 16 bit, but the signals are digitized at our stations by a sampling frequency of 20 Hz, with the same dynamic range. Table 1 shows the station name, epicentral distance, epicenter-to-station azimuth, maximum values of acceleration and velocity, and instrument type used at each station.

Figure 2 shows observed accelerograms (radial and transverse components) with distances. The S wave portion shows the maximum acceleration, but its attenuation with distance is not so simple. The frequency content of the signals and the duration of motion after S arrival are different from station to station. These facts represent the source, propagation path and site effects, which will be analyzed in detail in the following sections.

### 3. Source process

We estimated the focal mechanism of the earthquake using short period P wave first motions obtained by RCEP (Research Center for Earthquake Prediction) of Hokkaido University. Figure 1 shows P wave first motions and the

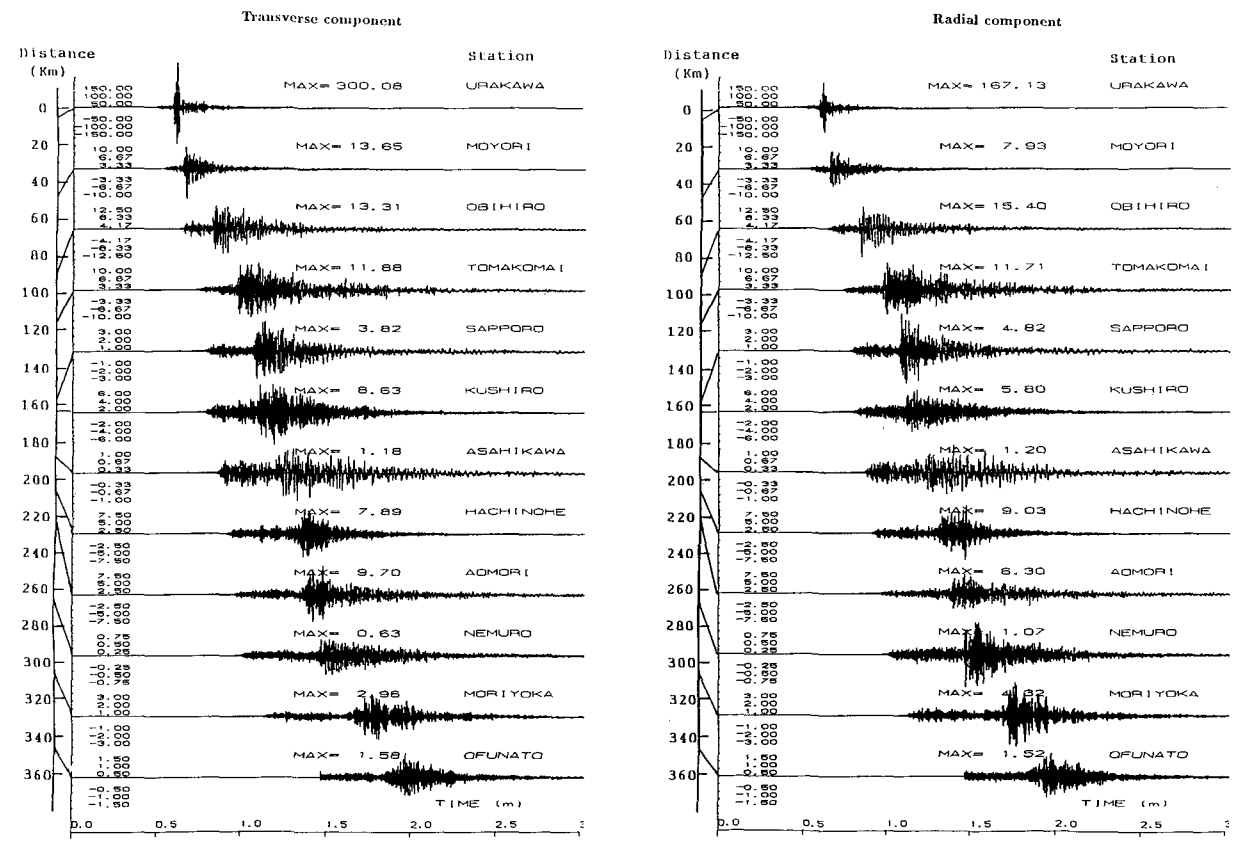


Fig. 2. Original transverse and radial accelerograms vs. distances.

focal mechanism obtained. This mechanism is approximately the same as obtained by Dziewonski et al. (1990). The Urakawa earthquake was caused by almost dip-slip (thrust) faulting with maximum pressure axes in the NE-SW direction.

We estimated seismic moment  $M_0$  from the area of P-wave displacement pulse,  $\mathcal{Q}_0$ , using the equation (e.g., Frankel, 1981)

$$M_0 = \frac{r\mathcal{Q}_0}{C}, \quad (1)$$

where  $r$  is hypocentral distance and  $C$  is a constant given by

$$C = \frac{F_s R_{\theta,\varphi}}{4\pi\rho\alpha^3}, \quad (2)$$

which includes the effects of the surface correction ( $F_s=2$ ),  $\rho$  and  $\alpha$  are average values of density and P wave velocity in the lithosphere; the values  $2.7 \text{ g/cm}^3$  and  $7.5 \text{ km/sec}$  have been used, respectively. We corrected the radiation pattern  $R_{\theta,\varphi}$  following Aki and Richards (1980).

Figure 3 shows P wave displacement time histories (vertical components) at Urakawa, Moyori and Obihiro stations. These were obtained by integrations of accelerogram and velocity seismograms in the frequency domain using the FFT method. P wave displacements show double pulses which may indicate the multiple shock (doublet) and the rupture duration of about 1.5 sec.

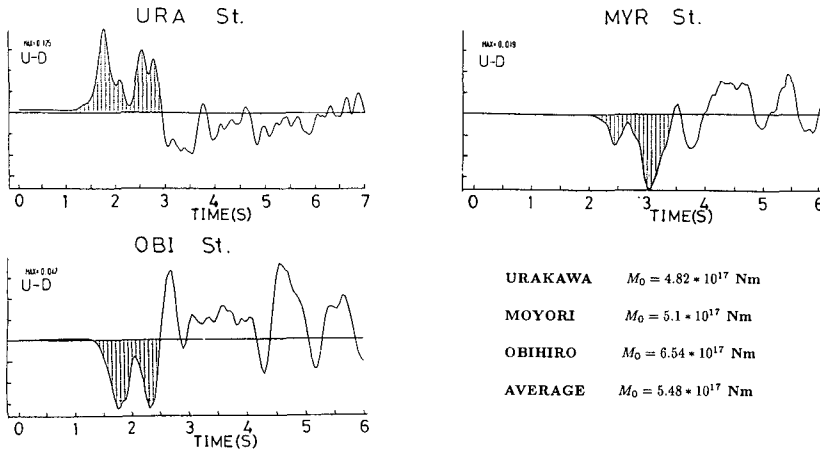


Fig.3. P wave displacement time histories (vertical components) of Urakawa, Obihiro and Moyori data recorded. The seismic moment at each station was estimated from shaded area.

The seismic moment at each station is shown in Fig. 3, and the average value is  $M_0 = 5.48 \times 10^{17}$  Nm. This value is about more than two times larger than that estimated from long-period seismic waves ( $M_0 = 2.1 \times 10^{17}$  Nm) by Dziewonski et al. (1990).

#### 4. Acceleration spectra

Fourier amplitude spectra were computed from accelerograms to study the character of the strong motion. For recorded velocity seismograms (Moyori and Obihiro) we obtained acceleration spectra by differentiating the velocity spectra in the frequency domain. Figure 4 illustrates the results for the transverse components of strong ground motion. They were obtained for the whole record as shown in Fig. 2. There was little difference between spectra for the transverse and radial components; then, the character of acceleration spectra was analyzed based on the results for the transverse components.

We can find conspicuous differences in spectral shape at high frequencies 1 to a corner frequency of anti-alias filter: 10 Hz and 8 Hz for JMA and ourselves recording system, respectively. The acceleration spectra may be classified into the following three types depending on the high frequency spectral shape. Type I: the spectrum has a sharp peak around 2 Hz (Urakawa and Morioka). Type II: the spectrum has the same but not so sharp peak around several Hz. (Kushiro, Hachinohe and Ofunato). Type III: the spectrum decreases with frequency, but the decay rate differs from station to station (Moyori, Obihiro, Tomakomai, Sapporo, Asahikawa, Aomori and Nemuro). The different spectral shapes may be attributed to different source, propagation path and site effects.

We should note that the acceleration spectra shown in Fig. 4 were obtained for the whole record. Before the interpretation of the different spectral shapes, we have to check what kinds of seismic waves dominate on each seismogram. To do this, we applied the multiple filter technique (Dziewonski et al. 1969) to the corresponding velocity seismograms; for recorded accelerograms, the velocity seismograms were obtained by integration in the frequency domain using the Fourier transform. We used the velocity seismograms for the multiple filter analysis to enhance relatively low frequency seismic waves. Instantaneous spectral amplitudes as a function of frequency and time are shown in Fig. 5 for each type of acceleration spectra. These figures indicate that S wave arrival dominates at high frequencies (1–10 Hz) for all types and that only for type III, low frequency (0.5 Hz) seismic waves dominate after S arrivals (also see Fig. 7).

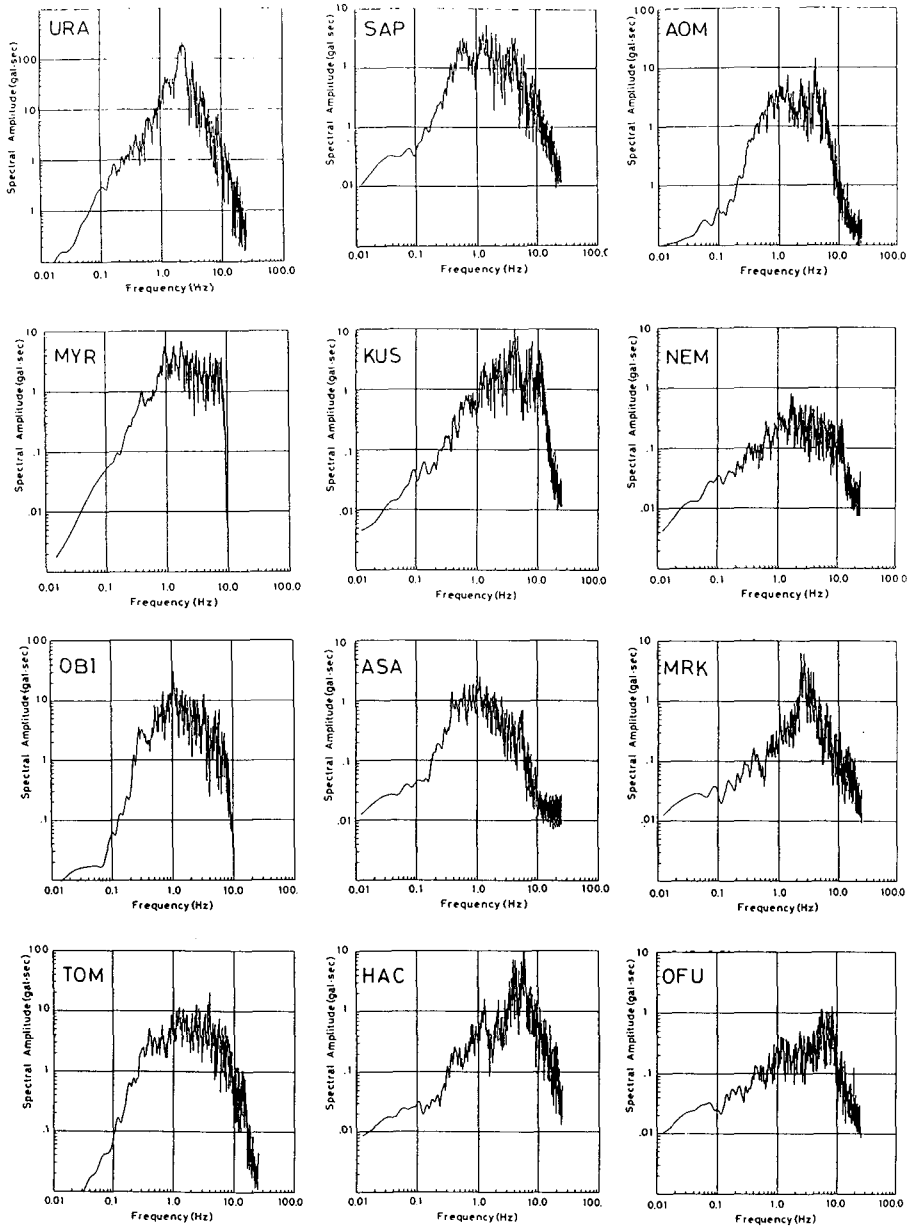


Fig. 4. Fourier acceleration spectra of transverse component data which were obtained for whole-record.

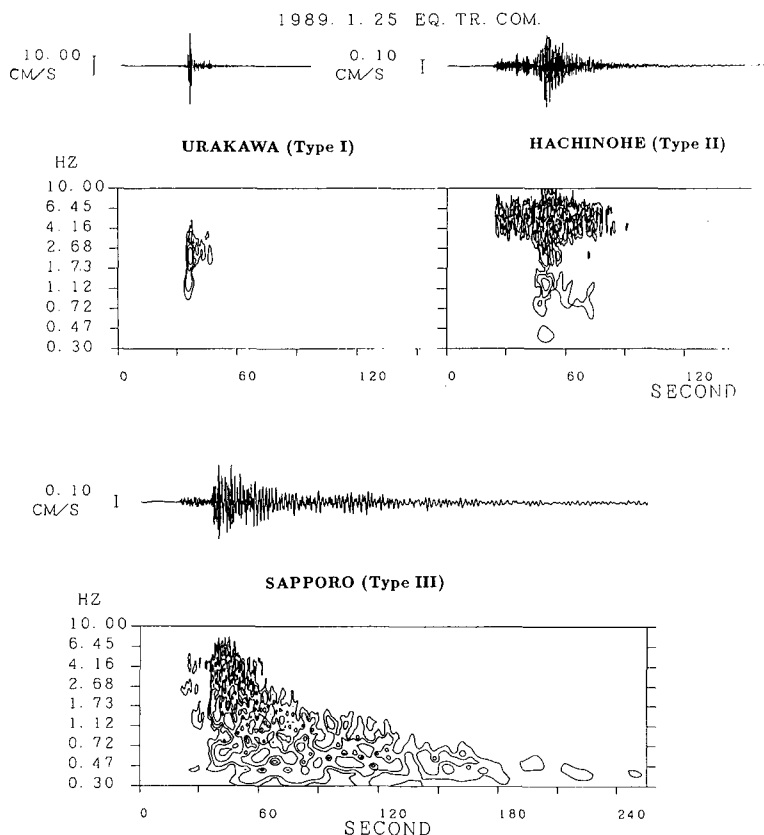


Fig. 5. Multiple filter analysis of velocity seismograms (transverse components) at Urakawa, Hachinohe and Sapporo stations. Contours of relative energy are shown at 6 db intervals.

From these facts we may conclude that although the acceleration spectra (Fig. 4) were computed for the whole record, they represent the spectra of S waves, at least, at high frequencies.

Now we interpret the different spectral shapes based on the  $\omega$ -square model, the spectrum of S-wave acceleration (Fig. 6). According to this model, the acceleration spectrum increases with  $f^2$  at low frequencies; and it is flat at high frequencies greater than the corner frequency (Aki, 1967; Brune, 1970; Hanks, 1982). Many observations showed that at high frequencies the spectrum of S-wave acceleration was characterized by a trend of exponential decay (e.g., Anderson and Hough, 1984; Rovelli et al., 1988) which was interpreted to be due to attenuation close to the observation site. The spectral shape of type III is

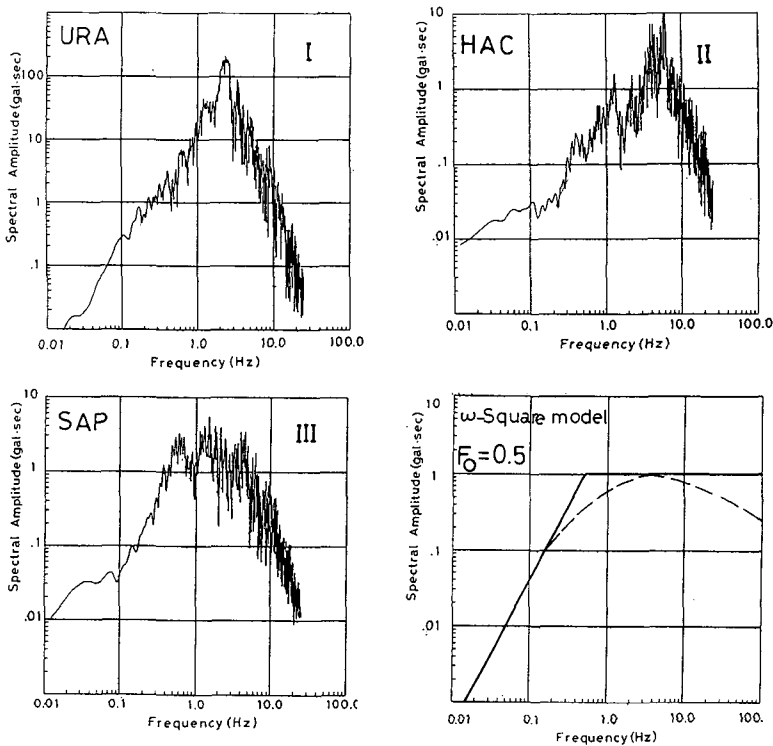


Fig. 6. Types I, II and III acceleration spectra and the  $\omega$ -square model, the spectrum of S-wave acceleration (a solid line represent the idealized spectrum and a dashed line, the actual spectrum including attenuation along the path).

very similar to the  $\omega$ -square model: we may assume the corner frequency ( $f_0$ ) of the Urakawa earthquake to be about 0.5 Hz based on the relation between the seismic moment and the corner frequency given by Takemura et al. (1991). On the contrary, the spectral shapes of type I and II deviate from this model. They show a sharp peak at about 2 or several Hz instead of exponential decay at high frequencies. These deviations are attributed to site resonances and peculiar amplifications (Anderson and Hough, 1984; Rovelli et al., 1988).

## 5. Attenuation of S waves

Here, we study attenuation of S waves due to propagation in the lithosphere. Previous studies (e.g., Aki, 1980) show that the spectral amplitudes of S waves can be described by

$$A(f, r) = \frac{A_0(f)}{r} e^{-\pi f \int \frac{dr}{Q(f)\beta}}, \quad (3)$$

where  $A_0(f)$  is source spectrum,  $r^{-1}$  is the contribution from geometrical spreading,  $Q(f)$  is the quality factor at frequency,  $f$ , and  $\beta$  is the S-wave velocity (we assumed a  $\beta = 4.0$  km/sec). We must note that above equation does not include the effect of radiation pattern. However, the radiation pattern effects on high frequency waves have not been observed definitely. If the  $Q(f)$  is independent of depth and constant along the path, an exponential term in equation (3) is given by  $\exp(-\pi f r / Q(f)\beta)$ . Then the logarithm of spectral amplitude (corrected for the geometrical spreading) versus distance ( $r$ ) should show a linear falloff with distance :

$$\ln(A(f, r)r) = \ln A_0(f) + \frac{-\pi f r}{Q(f)\beta}. \quad (4)$$

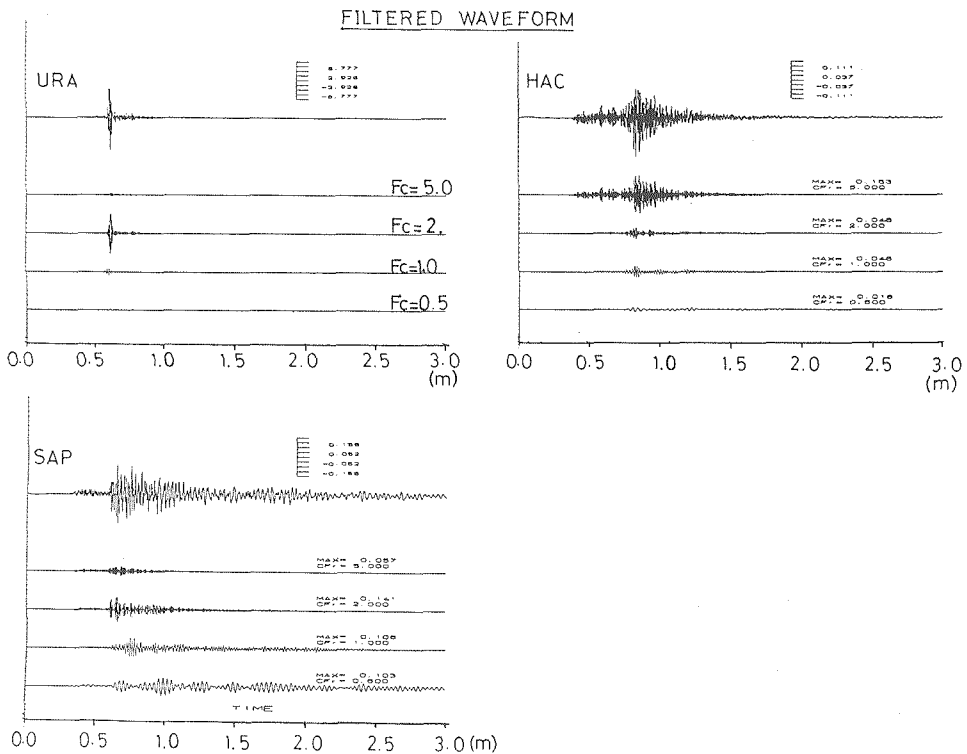


Fig. 7. An example of filtered waveforms at central frequencies ( $F_c$ ) of 0.5, 1.0, 2.0 and 5.0 Hz.

The slope of the linear falloff gives the  $Q(f)$  value.

We obtained the spectral amplitudes of S-waves from band-pass filtered velocity seismograms with central frequencies of 0.5, 1, 2, and 5 Hz. An example of the band-pass filtered seismograms is shown in Fig. 7. The spectral amplitudes of S waves were measured for transverse and radial components and the average of both values was used as data. Figure 8 shows the spectral amplitudes versus distance at discrete frequencies. Fluctuations of the amplitudes are somewhat large and may be attributed to no corrections for radiation

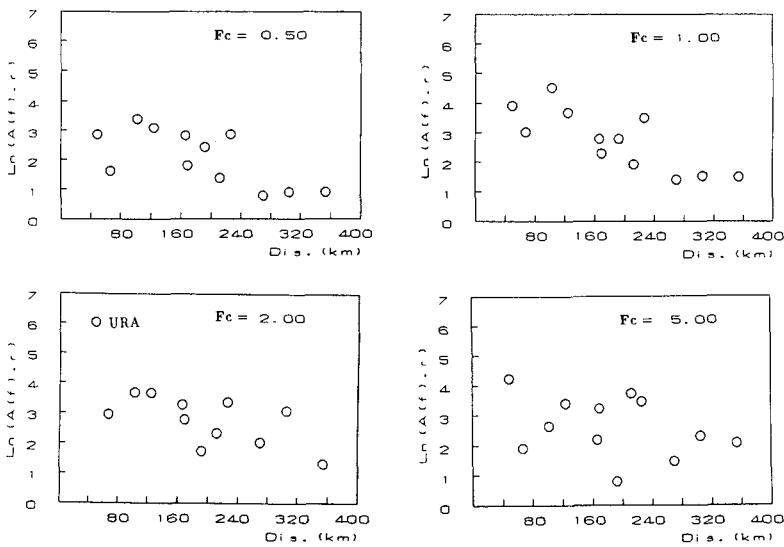


Fig. 8. Spectral amplitudes vs. focal distances at discrete frequencies 0.5, 1.0, 2.0 and 5.0 Hz. Each amplitude is the average of the transverse and radial components.

Table 2. Slops, their standard errors (SE) and quality factors (best estimation).

Central frequency	Slop	SE	Q
0.5	-0.00714	0.00458	55
1.0	-0.00939	0.00475	84
2.0	-0.00910	0.00632	172
2.0	-0.00559*	0.00510*	290*
5.0	-0.00377	0.00695	1040

\*=results obtained for data except Urakawa.

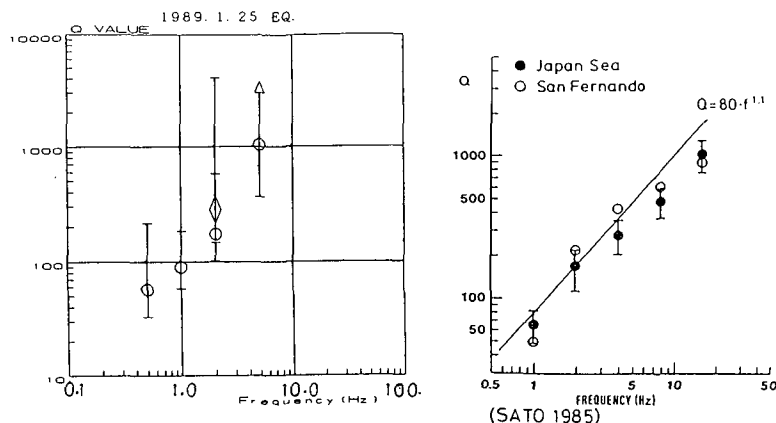


Fig.9. Obtained  $Q$  values plotted against frequency. Error bars show 95% confidence limits of the estimates. At central frequency of 2 Hz we obtained two results for different data sets: one is the data set including Urakawa (circle) and the other is the data set except Urakawa (diamond) (see Fig. 8). A triangle at 5 Hz indicates a very large error of estimated  $Q$  value. Also shown are the  $Q$  values obtained for the San Fernando earthquake of 1971, and for the Japan sea earthquake of 1983 (Figure after Sato (1985)).

pattern and site responses, but they show the linear falloff with distance. The linear regression was obtained by the least-squares method (Table 2). As mentioned in the previous section, the acceleration spectrum at Urakawa has a sharp peak around 2 Hz attributed to the site resonances. Actually the spectral amplitude at Urakawa at the central frequency 2 Hz is relatively large. Then at this central frequency, we obtained the results for two data sets; one is all data and the other, data except Urakawa station. The resulting values of  $Q(f)$  is shown in Fig. 9. Error bars show 95% confidence limits determined from residuals of regression by equation (4). The 95% confidence limits at 5 Hz was achieved with a large error of  $Q$ . Two data sets at the central frequency of 2 Hz yielded approximately the same  $Q$  value. The  $Q$  values increase with frequency as obtained by Aki (1980) and Sato (1985).

## 6. Discussion and conclusions

During the analysis of strong motion seismograms of the Urakawa earthquake we found two kinds of local site responses. One is excitation of long-period seismic waves (0.5 Hz) after S arrivals. The other is sharp peaks of acceleration spectrum at high frequencies. Here we compare these site

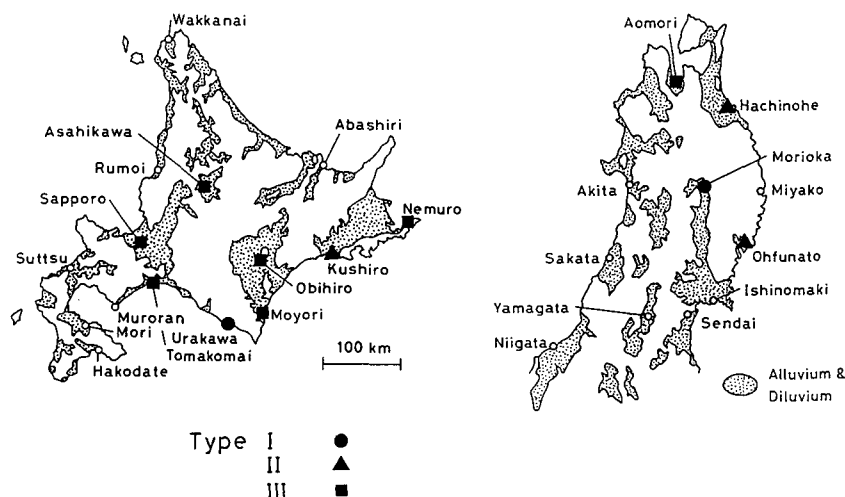


Fig. 10. Type of the acceleration spectrum at each station and a simple surface geology of Hokkaido and Tohoku districts.

responses with a simple surface geology of Hokkaido and Tohoku districts (Fig. 10). We observed long-period waves at many stations, except Moyori and Nemuro, belonging to spectral shape type III (Fig. 4). These stations are located on the alluvial plains having thick sedimentary layers; for example, Obihiro in the Tokachi plain and Sapporo and Tomakomai in the Ishikari plain. The basement structures to depths of a few kilometers beneath these plains have been obtained by Matsushima and Okada (1990) and Okada et al. (1990) using long-period microtremors. The structures obtained show the variation of the basement depths, that is, the irregularity of the sediment-basement interface. Then the long-period seismic waves may be surface waves locally generated on the irregular, sediment-basement interface due to the incident waves (Sasatani et al., 1991). Stations belonging to type I and II which show sharp peaks at high frequencies are located on rock sites and sedimentary plains (Fig. 10). We believe that sedimentary thickness at these stations is very thin to explain the high frequency resonances.

In conclusion, we studied the source, propagation path and site effects on strong ground motion from the Urakawa earthquake of Jan. 25, 1989. We observed two kinds of local site responses as mentioned above. Furthermore, we obtained  $Q$  values of  $S$  waves, which increase with frequency. However, more data have to be studied to obtain the definite conclusions.

### Acknowledgments

The authors are grateful to the staffs of JMA for the supply of accelerograms on which this work is based. This work could not have been performed without the kind help of Miss Mitsuko Ikeda and Dr. Takeshi Matsushima among others at our laboratory.

### References

- Aki, K., 1967. Scaling law of seismic spectrum. *J. Geophys. Res.*, **72**, 1217-1231.
- Aki, K., 1980. Attenuation of shear-wave in the lithosphere for frequencies from 0.05 to 25 Hz. *Phys. Earth Planet. Int.*, **21**, 50-60.
- Aki, K., and P.G. Richards, 1980. *Quantitative Seismology, Theory and Methods*. W.H. Freeman and Co.
- Anderson, J.G. and S.E. Hough, 1984. A model for the shape of the Fourier amplitude spectrum of acceleration at high frequencies. *Bull. Seism. Soc. Am.* **74**, 1969-1993.
- Brune, J.N., 1970. Tectonic stress and the spectra of seismic shear waves from earthquakes. *J. Geophys. Res.*, **75**, 4997-5009.
- Dziewonski, A., S. Bloch and M. Landisman, 1969. A technique for the analysis of transient seismic signals. *Bull. Seism. Soc. Am.* **59**, 427-444.
- Dziewonski, A.M., G. Ekstrom, J.H. Woodhouse and G. Zwart, 1990. Centroid-moment tensor solutions for January-March 1989. *Phys. Earth Planet. Inter.*, **59**, 233-242.
- Frankel, A., 1981. Source parameters and scaling relationships of small earthquakes in the northeastern Caribbean. *Bull. Seism. Soc. Am.* **71**, 1173-1190.
- Hanks, T.C., 1982. *f*<sub>max</sub>. *Bull. Seism. Soc. Am.*, **72**, 1867-1879.
- Hough, S.E., K.H. Jacob and P.A. Friberg, 1989. The 11/25/88, M=6 Saguenay earthquake near Chicoutimi, Quebec: Evidence for anisotropic wave propagation in northeastern North America. *Geophys. Res. Lett.*, **16**, 645-648.
- Joyner W. and David M. Boore, 1988. Measurement, characterization, and prediction of strong ground motion. *Proc. Earthquake Engineering and Soil Dynamics*. II, Park City, Utah, Geotechnical Div., Am. Soc. Civil Engineers 43-102.
- Matsushima, T. and H. Okada, 1990. Determination of deep geological structures under urban areas using long-period microtremors. *BUTSURI-TANSA (Geophys. Explor.)*, **43**, 21-33.
- Okada, H., T. Matsushima, T. Moriya and T. Sasatani, 1990. An exploration technique using long-period microtremors for determination of deep geological structures under urbanized areas. *BUTSURI-TANSA (Geophys. Explor.)*, **43**, 402-417 (in Japanese).
- Rovelli, A., O. Bonamassa, M. Cocco, M. Di Bona, and S. Mazza, 1988. Scaling laws and spectral parameters of the ground motion in active extensional areas in Italy. *Bull. Seism. Soc. Am.* **78**, 530-560.
- Sasatani T., 1990. Strong ground motions from intermediate-depth earthquakes: A study of site effects. *J. Fac. Sci. Hokkaido Univ., Ser. VII (Geophys.)*, **8**, 449-464.
- Sasatani, T., T. Matsushima and T. Koyanagi, 1990. Observation of strong motion in and around the Tokachi plain. *Geophys. Bull. Hokkaido Univ.*, **54**, 15-22 (in Japanese).
- Sasatani, T., M. Ikeda and N. Sakajiri, 1991. A study of site effects by means of strong-motion seismograms from near-by, intermediate- depth earthquakes. *J. Phys. Earth* (in press).
- Sato, T., 1985. Rupture characteristics of the 1983 Nihonkai-chubu (Japan sea) earthquake

as inferred from strong motion accelerograms. J. Phys. Earth, **33**, 525-557.

Takemura, M., T. Ikeura and T. Uetake. 1991. Evaluation of the relation between seismic moment and corner frequency from strong motion records. Abstr. Meet. Seismo. Soc. Jpn., No. 1, C21-04 (in Japanese).